

Location of Diphenylhexatriene (DPH) and Its Derivatives within Membranes: Comparison of Different Fluorescence Quenching Analyses of Membrane Depth[†]

Robert D. Kaiser and Erwin London*

Department of Biochemistry and Cell Biology and Department of Chemistry, State University of New York at Stony Brook, Stony Brook, New York 11794-5215

Received January 9, 1998; Revised Manuscript Received April 13, 1998

ABSTRACT: The average membrane location of a series of diphenylhexatriene (DPH)-derived membrane probes was analyzed by measuring the quenching of DPH fluorescence with a series of nitroxide-labeled lipids in which the depth of the nitroxide group is varied. All DPH derivatives were located deeply within the bilayer. Some derivatives were anchored at a shallower depth than free DPH by attachment to cationic or anionic groups. However, the absolute change in DPH depth upon attachment to such groups was relatively modest (<4 Å). In fact, protonated DPH fatty acid and a DPH fatty acyl group attached to a phosphatidylcholine were found to locate slightly more deeply than free DPH. The location of DPH derivatives can be explained by the length of the DPH group and its tendency to orient predominantly parallel to the fatty acyl chains of the bilayer. These factors allow a charged group attached to one end of a DPH molecule to be accommodated at the polar surface while maintaining a deep DPH location. Basically, it appears that most DPH derivatives probe the same region in the bilayer. We conclude previously reported differences in fluorescence polarization of free and anchored forms of DPH may reflect a direct effect of anchoring on motion rather than an effect on average DPH location. Other experiments showed the localization of DPH probes was found to be similar in the presence and absence of cholesterol. This implies that previously observed cholesterol-induced effects on DPH fluorescence polarization also largely reflect differences in DPH motion, not DPH location. From the quenching results it was also possible to define rules governing the location of a variety of chemical groups in membranes by comparison of the results obtained with DPH derivatives to those of similar derivatives of other fluorescent groups. Finally, an important goal of this study was to compare different methods of analysis of quenching data: parallax analysis, distribution (Gaussian) analysis (using a single Gaussian), and a second-order polynomial analysis. To evaluate the accuracy of these methods, the apparent depths of a series of fluorescence probes previously analyzed by parallax analysis was reanalyzed with all three methods. There was good agreement unless the fluorescent molecule was very shallow or very deep. In such cases, only parallax analysis gave physically reasonable results. This is likely to be due to the lack of a sufficient number of quenchers spanning a wide enough range for other analyses to compensate for deviations from ideal curves. Parallax analysis was also compared to distribution (Gaussian) analysis using a double Gaussian fit to account for quenching from the trans leaflet (Ladokhin, A. (1997) *Methods Enzymol.* 278, 462–473). Again more physically reasonable results were obtained from parallax analysis, likely due to non-Gaussian behavior of the depth dependence of quenching. Notwithstanding these observations, the significant number of cases where Gaussian curve fitting methods for quenching analysis are most powerful are discussed.

One of the fundamental questions involved in the study of membrane structure and function is, What chemical and structural factors control the depth of molecules in membranes? In addition to membrane proteins, a wide variety of hydrophobic and amphipathic compounds interact with and modulate the activity of voltage-gated ion channels, membrane-bound enzymes, and membrane-bound receptors. Also, many hydrophobic fluorophores are used as membrane probes for a variety of purposes, and the interpretation of their behavior depends in large part upon where they are

located in the bilayer. Thus, knowledge of molecular locations within membranes is important for understanding the structure/function relationship and useful for the rational design of membrane-inserting molecules.

Our group has developed a fluorescence quenching technique called parallax analysis, which allows the depth of a fluorescent group in a lipid vesicle to be determined from the result of two quenching experiments (1–3). In one experiment, the fluorescence intensity of a fluorophore in the presence of a nitroxide (spin)-labeled quencher locating at a specific depth is measured. In a second experiment, fluorescence is measured in the presence of a quencher carrying the nitroxide group at a different depth. The ratio of the two intensities is then substituted into an equation

[†] This work was supported by NIH Grant GM 48596.

* Author to whom correspondence should be addressed. E-mail: elondon@ccmail.sunysb.edu.

that allows calculation of depth at a high level of resolution. Parallax analysis has been applied to a large number of different fluorescent probes, polypeptides and proteins (1–10).

In this study, the depth of a series of DPH¹ probes was examined. These probes were chosen for a number of reasons. One was that it is important to know DPH depths to allow their more precise use as membrane probes. DPH and its derivatives are often the probes of choice for studies of the structure and dynamic properties of membranes (11, 12), and have been most often used to estimate membrane fluidity and/or order (13–19). DPH derivatives are ideal for such experiments because they exhibit a strong fluorescence increase upon binding to lipids and have sensitive polarization (anisotropy) responses to phospholipid orientational order (20). Derivatives of DPH are often chosen to probe different regions of the bilayer (15–18, 21–24), but their exact locations within the bilayer have not been determined (see Discussion), and it has been a constant ambiguity whether changes in DPH behavior due to its attachment to an anchoring group reflect changes in probe location or motional properties.

A second reason DPH probes were chosen was that there are a number of available DPH derivatives carrying various polar and charged groups. This allowed examination of the effect of such groups on membrane location. By comparing results with DPH to those with analogous derivatives of other fluorescent molecules we could eliminate effects due to fluorophore structure, allowing analysis of the relationship between depth and chemical structure.

Finally, we compared the performance of the parallax analysis with other methods of fluorescence quenching analysis. In most cases the parallax analysis gave the same results as other methods, but in other cases it is the only method that gives physically reasonable results. This represents a critical demonstration of the reliability of the parallax analysis. Other advantages and disadvantages of different analyses of fluorescence quenching are considered in detail.

EXPERIMENTAL PROCEDURES

Materials. DPH was purchased from Aldrich Chemical. DPH derivatives were purchased from Molecular Probes (Eugene, OR). The purity of the DPH probes was checked by TLC on silica gel plates (Silica gel H, Uniplate, Newark, DE) using solvent systems of 30/4 hexane/CHCl₃ (v/v) for DPH; 65/50/4 (v/v) CHCl₃/CH₃OH/water for DPH-PC; 80/1/4 methanol/acetic acid/water for TMA-DPH and TMAP-

DPH; and 25/15 CHCl₃/CH₃OH for DPH-propionic acid. Only TMAP-DPH showed any fluorescent impurities. After extraction of the spots from the TLC plate, it was found these impurities had a total of only 1% of the fluorescence of the TMAP-DPH spot.

Assay of Spin-Label Content of Spin-Labeled Lipids. Nitroxide-labeled PCs and DOPC were purchased from Avanti Polar Lipids (Pelham, AL). The purity of phospholipids was checked by TLC on silica gel plates as described previously (3). No impurities were detected on the lipids after the plates were sprayed with 40% sulfuric acid and charred. The concentration of phospholipids was determined by phosphate assay after total digestion (3). The actual nitroxide content of the nitroxide-labeled lipids was calculated from the intensities of the doubly integrated ESR spectra as described previously (1). Alternatively, the concentration of the spin-labeled lipids was assayed with fluorescence quenching by determining the percent of nitroxide-labeled lipid that had to be incorporated into vesicles to give the same quenching of anthroyloxy fatty acids as that found previously for vesicles containing 15% nitroxide-labeled lipids (3). The ratio of nitroxide groups to lipid was generally found to be in the range 0.6–0.9.

Preparation of Samples for Fluorescence Measurements. Depth measurements were made on samples containing DPH derivatives incorporated into 200 μ M unilamellar vesicles prepared by octylglucoside (OG) dilution (25). Solutions of 25 μ M DPH derivative in 25 mM OG were prepared by drying aliquots of OG and DPH derivatives dissolved in ethanol with N₂ gas and then dissolving in H₂O. In separate tubes, ethanol solutions containing 0.85 μ mol of OG and 170 nmol of total phospholipid containing either DOPC, or DOPC with 15 mol % 5-SLPC, 12-SLPC, or TempoPC² were mixed and then dried with N₂. Then 34 μ L of the DPH derivative in OG was added and the samples were vortexed to dissolve all the components. Last, 816 μ L of buffer (10 mM Na acetate/150 mM NaCl, pH 4.5; 10 mM Na phosphate/150 mM NaCl, pH 7; or 10 mM glycine/150 mM NaCl, pH 10) was added to each tube and the tubes were vortexed for 30 s. The pH 7 buffer was used for all DPH derivatives except DPH propionic acid. This procedure gave a final lipid concentration of 200 μ M, which was a high enough concentration to give near-maximal DPH fluorescence and high enough so all fluorescence arose from DPH that was membrane bound (data not shown). Samples containing cholesterol were prepared identically except an additional 85 nmol of cholesterol was included with the phospholipid.

Fluorescence Quenching Measurements. Fluorescence was measured in 1 cm path length quartz cuvettes using a Spex Fluorolog spectrofluorimeter operating in ratio mode. The excitation and emission slits were set at 1.25 mm (2.3 nm band-pass) to prevent overloading of the photomultiplier tube. The excitation wavelength was set at 359 nm, and emission at 427 nm. To avoid photoisomerization of the DPH molecules, intensity measurements were limited to three consecutive 1 s readings, which were then averaged. Control

¹ Abbreviations: DOPC, 1,2-dioleoyl-*sn*-glycero-3-phosphocholine; DPH, 1,6-diphenyl-1,3,5-hexatriene; DPH-propionic acid, 3-[(4-(6-phenyl)-1,3,5-hexatrienyl)]phenylpropionic acid; DPH-PC, 1-palmitoyl-2-(3-(diphenylhexatrienyl)propanoyl)-3-palmitoyl-*sn*-glycero-3-phosphocholine; ESR, electron spin resonance; MLV, multilamellar vesicles; NBD, 7-nitro-2,1,3-benzoxadiazol-4-yl; NMR, nuclear magnetic resonance; OG, *n*-octyl- β -D-glucopyranoside (octyl glucoside); PC, 1,2-diacyl-*sn*-glycero-3-phosphocholine; 5- or 12-SLPC, 1-palmitoyl-2-(5- or 12-doxyl)stearoyl-*sn*-glycero-3-phosphocholine; SUV, small unilamellar vesicles; Tempocholine, 4-(*N,N*-dimethyl-*N*-(2-hydroxyethyl))-ammonium-2,2,6,6-tetramethylpiperidine-1-oxyl; TempoPC, 1,2-dioleoyl-*sn*-glycero-3-phosphotempocholine; TMA-DPH, 1-(4-trimethylammoniumphenyl)-6-phenyl-1,3,5-hexatriene; TMAP-DPH, *N*-((4-(6-phenyl)-1,3,5-hexatrienyl)phenyl)propyl)trimethylammonium; TLC, thin-layer chromatography.

² The nitroxide-labeled lipid contains some molecules that lack a nitroxide group. The amount of nitroxide-labeled lipid is adjusted to give 15% nitroxide-containing molecules and 85% other lipid molecules (DOPC plus inactive quencher).

experiments showed that fluorescence intensities were stable over this time and that preincubation in the dark or in room light did not affect intensity (data not shown). The fluorescence intensity from triplicate samples containing fluorophore was averaged. The intensity of the background samples without fluorophore was found to be negligible (<1%). All measurements were made at room temperature. F/F_0 , the ratio of the fluorescence intensities in the presence (F) to that in the absence (F_0) of the nitroxide-labeled lipids was calculated and substituted into the parallax equation (1, 3) to calculate DPH depth (see below).

To confirm the absence of reactivity between nitroxide-labeled lipids and DPH probes, fluorescence was measured after 100 μ L aliquots of each sample were dissolved in 900 μ L ethanol. This abolished quenching and equal fluorescence intensities were observed in samples with and without nitroxide-labeled lipids.

To see whether quenching was stable, quenching in vesicles containing DPH propionic acid vesicles at pH 4.0 was measured twice, 9 days apart, incubating samples at 4 °C in the dark between measurements. After 9 days, a slight decrease quenching was observed. The decrease was similar for all three quenchers, and the calculated depth did not change significantly.

Calculation of Depth by Parallax Analysis. Using F/F_0 values measured as described above, the distance of fluorophores from the center of the bilayer was calculated using the parallax equation (1, 3):

$$z_{cf} = L_{c1} + (-\ln(F_1/F_2)/\pi C - L_{21}^2)/2L_{21}$$

where z_{cf} is the average distance of the fluorophore from the center of the bilayer, F_1 is the fluorescence intensity (F/F_0) in the presence of the shallow quencher (quencher 1), F_2 is the fluorescence intensity (F/F_0) in the presence of the deeper quencher (quencher 2), L_{c1} is the distance of the shallow quencher from the center of the bilayer, L_{21} is the distance between the shallow and deep quenchers, and C is the concentration of quencher in molecules/ \AA^2 = (mole fraction of nitroxide-labeled phospholipid/area per phospholipid) = (mole fraction nitroxide/70 \AA^2) (1). The quenching by the pair of quenchers (i.e., nitroxide-labeled lipid) that quench the most (i.e., the TempoPC/5 SLPC pair or 5 SLPC/12SLPC pair) was used to calculate z_{cf} (3). The values used for the distances of the nitroxide group from the bilayer center were 5.85 \AA for 12SLPC, 12.15 \AA for 5SLPC, and 19.5 \AA for TempoPC (1, 3).

In model membranes containing cholesterol, the (lateral) concentration of nitroxide-labeled lipid and the depth of the quenchers in the membranes are altered. These values were calculated by assuming that 33 mol % cholesterol results in a 10% increase in the width of the acyl chain region of the bilayer, and that a cholesterol molecule occupies a lateral area of 32 \AA^2 (26, 27). The resulting value for C is (mole fraction of nitroxide-labeled phospholipid relative to total lipid including cholesterol)/[0.67(70 \AA) + 0.33(32 \AA)] = (mole fraction nitroxide/57.5 \AA^2), and the calculated values for the distances of 12SLPC, 5SLPC, and TempoPC nitroxides from the bilayer center were 6.45, 13.4, and 21 \AA , respectively. A similar process was used to estimate the change in depths of individual acyl chain carbon atoms (1) upon addition of cholesterol.

Calculation of Depth by Gaussian and Polynomial Analysis. Depth was also calculated using two alternate methods. One was the Gaussian distribution analysis method of Ladokhin and Holloway (28). In this method quenching is fit to the equation

$$-\ln F/F_0 = C[S/(\sigma[2\pi]^{1/2})]\exp(-0.5[(z-z_{cf})/\sigma]^2)$$

where z is the distance of the quencher from the center of the bilayer, σ is the parameter giving the width of the quenching distribution function as a function of depth, and S is the area, a measure of total sensitivity to quenching. The other method used was a simple second-order polynomial fit. We fit the dependence of F/F_0 as a function of z to the equation $F/F_0 = az^2 + bz + c$. In both cases the Slidewrite 3.0 program (Advanced Graphics Software, Carlsbad, CA) was used to fit the variable parameters and solve for z_{cf} . (Since F/F_0 is a minimum when the quencher and fluorophore are at the same depth, i.e., when $z = z_{cf}$, z_{cf} is the value of z at which the derivative of the fitting equation equals zero, e.g. for the polynomial equation $z_{cf} = -b/2a$.)

pH Titration Experiments. A buffer of 10 mM Na acetate/150 mM NaCl buffer, generally at pH 5.0, was titrated to pH 3 with a small amount of 1 M HCl. Samples containing 1 μ M DPH-propionic acid, 2 mM OG, and 200 μ M DOPC were prepared in this buffer. The solution was placed in a 1 cm quartz cuvette, and fluorescence was measured. Successive aliquots of base (NH_4OH) were added to increase pH and fluorescence was remeasured with about 1–2 min between readings.

Estimating the Depth of Functional Groups. To calculate the depth of functional groups, we first calculated the length of 1,6-DPH, which was estimated to be about 14 \AA between carbon atoms at each end using the Hyperchem program (Hyperchem, Inc., Gainesville, FL). In the liquid crystalline phase the distribution of an anchored DPH group in the bilayer has been roughly estimated to be within a cone with a $\theta_{\max} = 35^\circ$ from the bilayer normal (13, 29). A simple Gaussian distribution over all allowed angles would give an average orientation of 17.5° . Alternately, assuming a totally random distribution of DPH molecules at all angles would give an average angle of 25° (i.e., this corresponds to the solid angle containing half of the total possible DPH orientations). This results in a range for the average difference in depth of the ends of a DPH molecule of 12.7–13.4 \AA . Thus on the average, the depth of the center of the DPH group should be about $13/2 = 6.5$ \AA different from that of each end.

It appears that nitroxide quenching is dominated by an electron exchange process and thus is dependent on the degree of orbital overlap between that containing the excited state electron of the fluorophore and that of the unpaired electron of the nitroxide group (although close contact is not required) (30). Therefore, as previously, we approximate z_{cf} measured by nitroxide quenching as the depth of the center of the conjugated double bond system of the DPH molecule which should approximate the depth of the excited state electron.

The distance of a functional group from the bilayer center could then be estimated to be the sum of the distance of the shallow end of the DPH group from the bilayer center (Z_{cf}

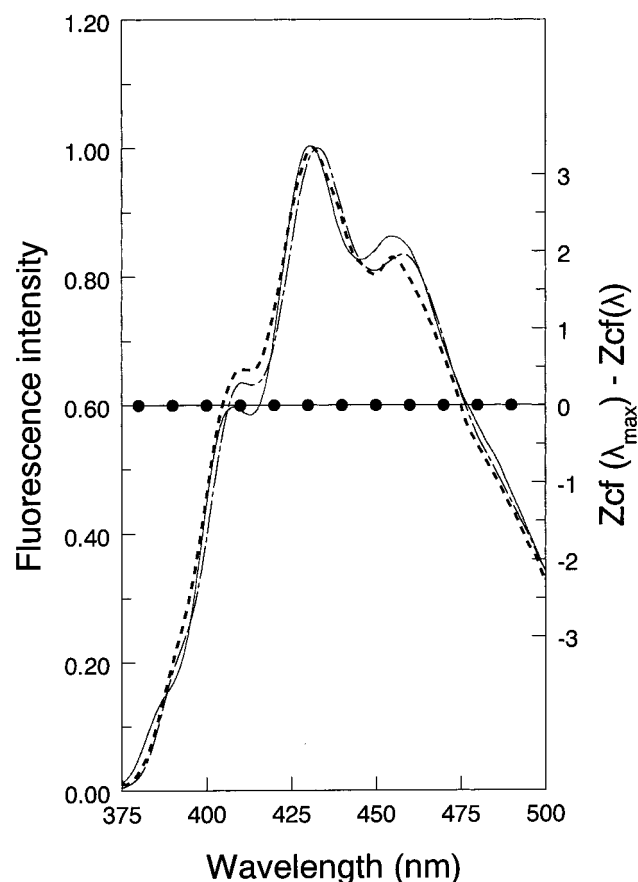


FIGURE 1: Emission spectra of DPH derivatives and effect of wavelength on Z_{cf} . (—), emission spectrum of DPH; (---), emission spectrum of DPH-PC; (---), emission spectrum of TMA-DPH. TMAP-DPH and DPH-propionic acid gave emission spectra identical to that of DPH-PC. Filled circles show the difference between Z_{cf} at λ_{max} and other wavelengths for DPH.

+ 6.5 Å) plus the calculated length of spacer between the DPH and its functional group. As previously, it was assumed for the spacer groups that CH_2 groups are on the average 0.9 Å apart in depth, as has been found for CH_2 groups on fatty acyl chains of lipids [see refs in (1)] and anthroyloxy fatty acids (3).

RESULTS

Measurement of Fluorescence Quenching: DPH Groups Locate Deep within the Bilayer. The location of a series of DPH derivatives in membranes was examined by fluorescence quenching. These molecules exhibited very similar emission spectra (Figure 1). Fluorescence was measured in unilamellar vesicles³ containing DOPC or DOPC mixed with 15% of shallow (TempoPC), medium (5SLPC), or deep (12SLPC) nitroxide-labeled lipids (Table 1). Strong fluorescence quenching was observed for all DPH derivatives. The amount of quenching obtained with the different nitroxide-labeled lipids was then used to calculate the distance of the fluorophores from the center of the bilayer (Z_{cf}) using the parallax equation (see Experimental Procedures). Table 1 shows the depth of DPH derivatives in model membrane vesicles. Overall, DPH derivatives are relatively deeply

Table 1: Nitroxide Quenching and Depth of Fluorophores in PC Vesicles

fluorophore	F_{TC}/F_o^a	F_5/F_o	F_{12}/F_o	Z_{cf}	D_{carbon}^b	Z_{group}^c
DPH (pH 7.0)	0.27	0.23	0.20	7.8	5.5	n/a
TMA-DPH (pH 7.0)	0.53	0.40	0.47	10.9	9	18.7
TMAP-DPH (pH 7.0)	0.36	0.26	0.26	8.9	7	19.4
DPH-PC (pH 7.0)	0.35	0.28	0.23	6.9	4.5	16.5
DPH-propionic acid (pH 4.5)	0.36	0.30	0.23	5.7	3	15.3
DPH-propionic acid (pH 10)	0.37	0.29	0.30	9.5	7	19.1

^a In general, F/F_o values are an average obtained from four samples. Average standard deviation of F/F_o values was about 0.02. The standard deviation in Z_{cf} values was 1.0 Å. ^b D_{carbon} gives the depth of the carbon atom on an underivatized 2-position fatty acyl chain equivalent to that of Z_{cf} . ^c Z_{group} is the estimated distance between the anchoring group attached to DPH and the center of the bilayer. For TMA and TMAP derivatives this is the nitrogen depth, and for the other derivatives it is that of the C of the propionic carboxyl group. n/a, not applicable.

Table 2: Nitroxide Quenching and Depth of Fluorophores in PC/Cholesterol Vesicles

fluorophore	F_{TC}/F_o^a	F_5/F_o	F_{12}/F_o	Z_{cf}	D_{carbon}	Z_{group}
DPH (pH 7.0)	0.37	0.30	0.23	6.7	4	n/a
TMA-DPH (pH 7.0)	0.54	0.42	0.45	10.7	8	18.5
TMAP-DPH (pH 7.0)	0.44	0.34	0.29	8.2	5.5	18.7
DPH-PC (pH 7.0)	0.46	0.36	0.27	6.2	3.5	15.8
DPH-propionic acid (pH 4.5)	0.45	0.37	0.24	4.6	2	14.2
DPH-propionic acid (pH 10)	0.41	0.33	0.31	9.2	7	18.8

^a In general, F/F_o values are an average obtained from four samples. Average standard deviation of F/F_o values was about 0.02. The average standard deviation in Z_{cf} was 0.5 Å. See Table 1 for other details.

buried within the acyl chain region of the bilayer, with an average distance from the bilayer center (Z_{cf}) of 6–11 Å.

In previous studies on other fluorescent probes, a small but significant effect of emission wavelength on measured depth was observed (3, 4). No significant effect of emission wavelength on DPH depth was found (Figure 1).

Depth of Cationic DPH Derivatives. We first examined the behavior of cationic DPH derivatives. The DPH group of trimethylamino (TMA)-DPH, in which the cationic TMA group is attached directly to one DPH phenyl ring, was located 3 Å more shallowly than free DPH ($Z_{cf} = 11$ Å vs 8). As charged groups locate shallowly in membranes (3, 4), anchoring of the DPH group of TMA-DPH at a shallower location would be predicted (22), although the exact location of the DPH group has been difficult to determine (see Discussion). The effect of anchoring in the case of trimethylaminopropyl (TMAP)-DPH ($Z_{cf} = 9$ Å) was much less than for TMA-DPH. This can be explained by the presence of the propyl spacer between the charged TMA group and DPH in TMAP-DPH. This should allow the TMA group to remain near the membrane surface without having to pull the DPH group to a significantly shallower depth.

Depth of DPH Fatty Acid and Fatty Acyl Derivatives. To examine the behavior of anionic DPH derivatives, DPH-propionic acid was examined. This probe has an ionizable carboxyl group, and the pH dependence of its depth exhibited a pK_a at about 7 (not shown). A similar value was estimated previously from the pH dependence of its fluorescence intensity and polarization (31), and is in agreement with values previously obtained for carboxyl ionization of other

³ We have repeatedly found the depth of small fluorescent probes is not affected by the size or curvature of the model membrane vesicles used (1, 5, 6).

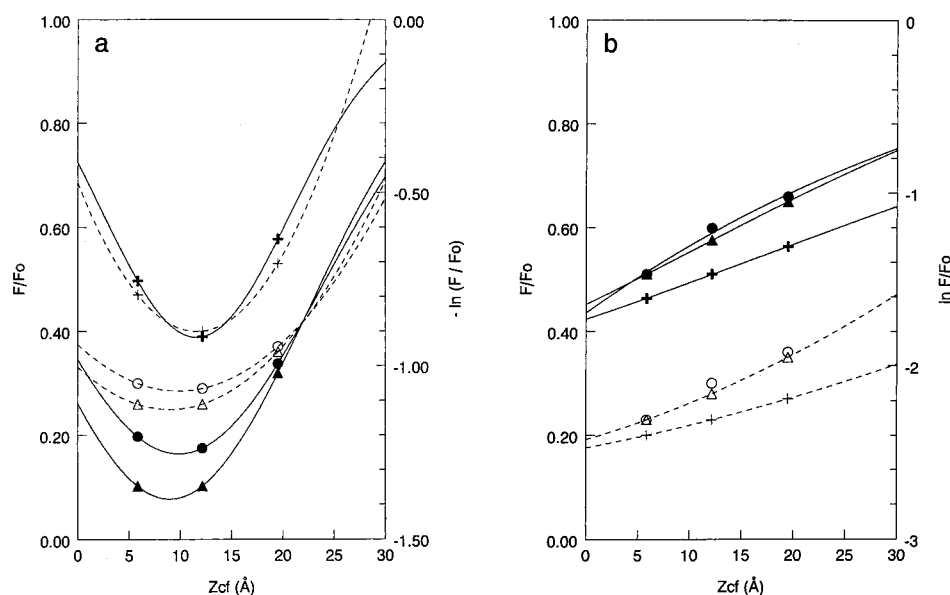


FIGURE 2: Curve fitting analyses of the Depth of DPH Derivatives. (a) (+), TMA-DPH; (open triangle), TMAP-DPH; (○), DPH propionic acid, pH 10. (b) (+), DPH; (open triangle), DPH-PC; (○) DPH-propionic acid, pH 5. (—) and right axis, distribution (Gaussian) analysis. (---) and left axis, polynomial analysis.

membrane-inserted fatty acids (2). Therefore, the depth of DPH-propionic acid at pH 5 ($z_{cf} = 5.7$) is that of the protonated form, and depth at pH 10 ($z_{cf} = 9.5$) is that of the ionized form (DPH-propionate). These depths indicate that ionized carboxyl anchors the DPH group at a significantly shallower location than the depth at which the carboxyl is protonated.

What seemed more surprising was that in the protonated state, DPH-propionic acid actually appeared to locate slightly more deeply than free DPH. This was a reproducible observation, as illustrated by the fact it was also observed in samples with cholesterol (Table 2). In this case, the spacer may push the DPH probe to a deeper location (see Discussion).

The behavior of the DPH-propionic acid esterified to the 2-carbon of PC (DPH-PC) was also examined. The DPH on DPH-PC was found to be intermediate in depth between that in the ionized and protonated forms of the free DPH fatty acid.

Depth of Polar and/or Charged Anchoring Groups. From the depth of the DPH derivatives and estimates for the average degree of tilt of DPH molecules, the depth of the polar and/or charged anchoring group attached to each DPH derivative can be roughly estimated (see Experimental Procedures). In the case of those DPH derivatives with charged groups, distances about 19 Å from the bilayer center were calculated (Table 1). The protonated carboxyl group locates close to 15 Å from the bilayer center.

Effect of Cholesterol on Quenching and Depth of DPH Derivatives. DPH derivatives have often been used to examine the effect of cholesterol on membrane fluidity using polarization (14, 24, 29). It is possible that some fraction of the effect of cholesterol on polarization reflects a change in DPH location. To examine whether this was the case, the depths of the DPH probes were remeasured in DOPC vesicles containing 33 mol % cholesterol. Table 2 shows that the quenching pattern observed in the presence of cholesterol was very similar to that observed in its absence. However, in general, quenching levels were more widely

dispersed in the presence of cholesterol. For example, the difference between F/F_0 for DPH quenching by TempoPC and 12SLPC is twice as large in the presence of cholesterol as in its absence. Similar quenching differences in the presence or absence of cholesterol were observed for most of the DPH derivatives. An increased dependence of the degree of quenching on quencher depth in the presence of cholesterol has also been seen previously for brominated lipid quenching of pyrene-labeled lipids (see Discussion).

Nevertheless, there was little effect of cholesterol on the depths of any of the DPH-derivatives (compare Tables 1 and 2).⁴ At most, the DPH derivatives may have located the equivalent of one carbon atom deeper in the presence of cholesterol. This contrasts with the large effect cholesterol can have on the location of hydrophobic α -helices under some conditions (6).

Comparison of Different Analyses for the Determination of Depth from Fluorescence Quenching Studies. Recently, alternate methods have been suggested for the analysis of fluorescence quenching data (28, 32, 33). These fit the dependence of quenching on quencher depth to Gaussian curves. To evaluate such methods, we compared the depth of DPH derivatives with parallax analysis and the Gaussian distribution analysis method of Ladokhin and Holloway (28). We also calculated the depths determined with a simple second-order polynomial curve to see if the apparent depth is sensitive to the exact form of the equations used to fit the quenching data, i.e., whether a Gaussian form was needed or whether a different smooth curve with a distinct point of minimum fluorescence could also fit the data.

⁴ There is very little difference when the corrections (see Experimental Procedures) for quencher depth and concentration in the presence of cholesterol are omitted (without the corrections z_{cf} values were about 1 Å deeper). Therefore, the results are not sensitive to the precision of these corrections. In addition, it should be noted that the same depths and effect of cholesterol on quenching were found for DPH incorporated into multilamellar vesicles (MLVs) (not shown). Therefore, the effect of cholesterol appears to be independent of sample preparation method.

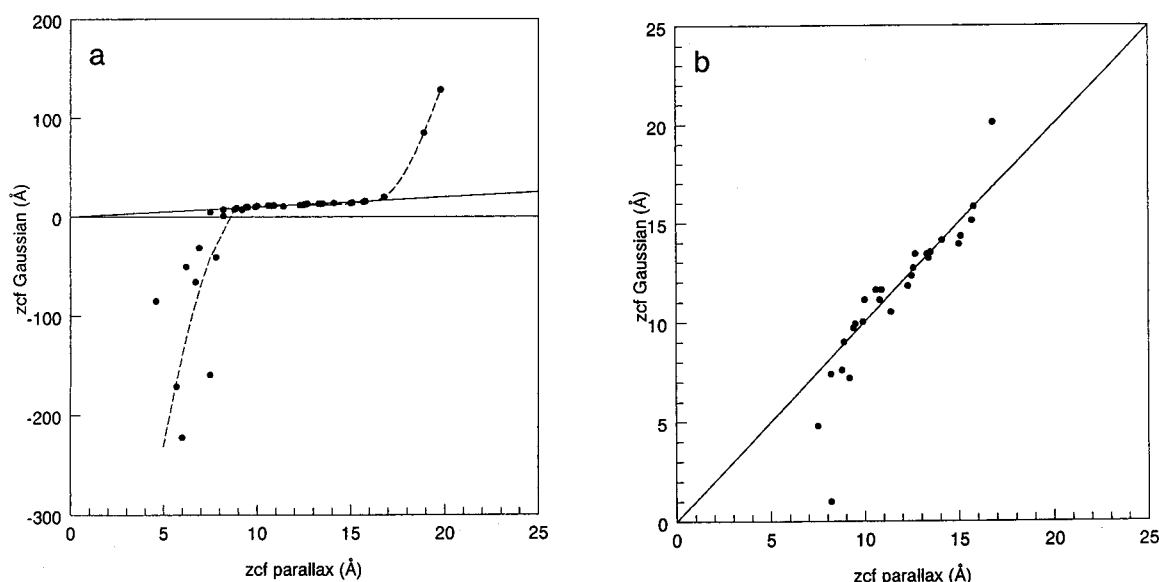


FIGURE 3: Correlation between z_{cf} determined by parallax analysis and distribution (Gaussian) analysis. (a) All values from Tables 3 and 4. (b) Expanded view for fluorophores closest to the quenchers.

Table 3: Comparison of Average Depth of DPH Probes Determined by Different Quenching Analyses^a

fluorophore	Z_c parallax	Z_{cf} polynomial	Z_{cf} distribution (Gaussian)
TMA-DPH	10.9	11.7	11.6
TMAP-DPH	8.9	9.0	9.0
DPH-propionic acid (pH 10.0)	9.5	9.9	9.9
1,6-DPH	7.8	-38.8	-41.0
DPH-PC	6.9	-25.1	-31.5
DPH propionic acid (pH 4.5)	5.7	NF ^b	-170.7
TMA-DPH with cholesterol	10.7	10.5	11.4
TMAP-DPH with cholesterol	8.2	-0.5	1.0
DPH propionic acid (pH 10.0) with cholesterol	9.2	6.2	7.2
1,6-DPH with cholesterol	6.7	NF	-65.3
DPH-PC with cholesterol	6.2	NF	-50.6
DPH propionic acid (pH 4.5) with cholesterol	4.6	NF	-85.2

^a Quenching data from Tables 1 and 2 were reanalyzed with a second-order polynomial and distribution analysis. ^b NF = no fit, polynomial analysis could not fit to a curve in which F/F_0 had a minimum value. For the Gaussian analysis, a coefficient of determination for the curve fitting very close to 1 was obtained in all cases.

Figure 2 illustrates the results obtained for DPH derivatives with curve-fitting methods. z_{cf} values were obtained from the depth at which these curves reached a minimum. The comparison between z_{cf} determined by parallax analysis and curve-fitting analyses for DPH derivatives is summarized in Table 3. The agreement is excellent (within 1 Å) where the quenching by 5SLPC was equal or stronger than that by 12SLPC. Where quenching by 12SLPC was stronger than that by 5SLPC, both Gaussian and polynomial methods give physically meaningless values (depths of $z_{cf} < 0$, deeper than the center of the bilayer). In some of these cases, no fit giving a z_{cf} value could be derived from the polynomial analysis.

To see if these conclusions could be generalized to other fluorescent probes, parallax analysis and the curve-fitting methods were compared for anthroyloxy, NBD, anthracene, carbazole, indole, and phenol derivatives (1–4). The resulting z_{cf} values are summarized in Table 4. Figure 3 shows

Table 4: Comparison of Average Depth Determined by Different Quenching Analyses^a

fluorophore	Z_{cf} parallax	Z_{cf} polynomial	Z_{cf} distribution (Gaussian)
anthracene	9.9	10.1	10
anthracenemethanol	12.7	13.3	13.4
anthracenemethyl	1.4	NF	-60.2
bisnorhydroxycholelate (AMC)			
AMC acetate	7.5	5.0	4.8
AMC oleate	12.6	12.7	12.7
anthracene propionic acid	10.0	11.1	11.1
anthracenylpropyl ammonium chloride	10.8	9.7	11.1
anthracenylpropyl trimethylammonium bromide	13.3	13.3	13.4
2-anthroyloxy stearate (pH 10)	16.8	20.0	20.1
2-anthroyloxy stearate (pH 5)	15.8	15.8	15.8
6-anthroyloxy stearate (pH 5)	12.3	11.8	11.8
6-anthroyloxy stearate (pH 10)	15	13.9	13.9
9-anthroyloxy stearate (pH 5)	8.8	7.6	7.6
9-anthroyloxy stearate (pH 10)	12.6	12.7	12.7
12-anthroyloxy stearate (pH 5)	6.0	NF	-221.9
12-anthroyloxy stearate (pH 10)	7.5	NF	-159
carbazole	15.1	14.4	14.3
11-carbazole undecanoic acid (pH 5)	7.5	4.9	4.8
11-carbazole undecanoic acid (pH 10)	10.6	11.6	11.6
indolebutyric acid	15.7	15.0	15.1
methylaminomethyl anthracene	12.5	12.4	12.3
methylanthracene	8.2	7.5	7.4
methyl anthracene propionate	9.4	9.7	9.7
methylcarbazole	13.4	13.2	13.2
NBD-PE	18.9	NF	84.9
12-NBD-PC	19.8	NF	128.4
octylphenol	14.1	14.3	14.1
tryptophan octyl ester	13.5	13.5	13

^a Quenching of various probes by TempoPC, 5SLPC, and 12SLPC in PC vesicles (3–5) was reanalyzed by parallax, second-order polynomial, and distribution analysis.

the correlation between the z_{cf} calculated by different methods. Excellent agreement among all three methods is obtained when quenching by 5SLPC is stronger than that by 12SLPC and TempoPC ($9 \text{ Å} < z_{cf} < 16 \text{ Å}$).⁵ However,

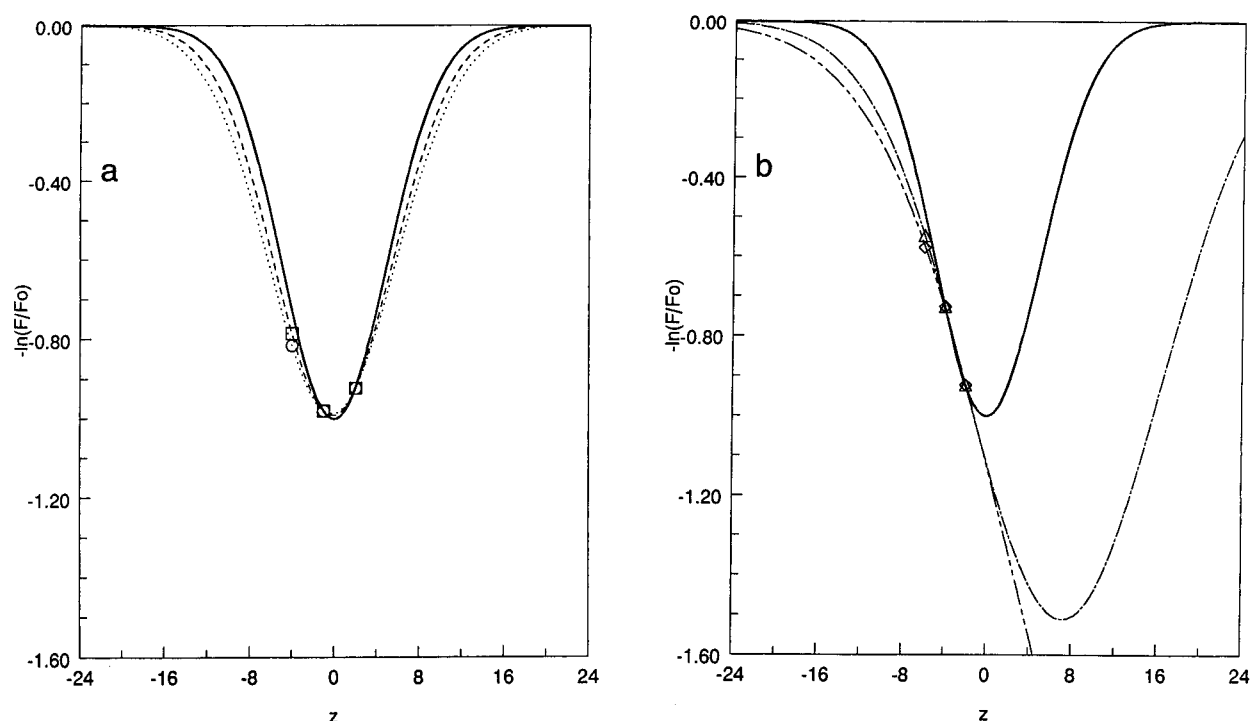


FIGURE 4: The effect of deviations from ideal values on the ability to determine Z_{cf} from a curve fitting analysis. (a) The effect of a deviation from a Gaussian when the quenchers are located close to fluorophore depth. Quenchers at z (difference in fluorophore and quencher depth) equals -4 , -1 , and $+3$ Å. (—), Gaussian dependence of $\ln F/F_0$ on z (difference in depth between quencher and fluorophore) for F/F_0 minimum = 0.37 and $\sigma = 5$ Å. In this case, the quencher at $z = -4$ Å gives $F/F_0 = 0.48$. (---), Gaussian fit when quencher at $z = -4$ Å gives $F/F_0 = 0.46$. (·····), Gaussian fit when quencher at $z = -4$ Å gives $F/F_0 = 0.44$. Notice the lack of an effect on apparent Z_{cf} ($= z$ at F/F_0 minimum). (b) The effect of a deviation from a Gaussian when quenchers are all located more shallowly or deeper than fluorophore depth. Quenchers at $z = -6$, -4 , and -2 Å. (—) Gaussian dependence of $\ln F/F_0$ on z for F/F_0 minimum = 0.37 and $\sigma = 5$ Å. In this case, the quencher at $z = -6$ Å gives $F/F_0 = 0.61$. (---), Gaussian fit when quencher at $z = -6$ Å gives $F/F_0 = 0.58$. (·····), Gaussian fit when quencher at $z = -6$ Å gives $F/F_0 = 0.56$. Notice large effect of F/F_0 at -6 Å on apparent Z_{cf} ($= z$ at F/F_0 minimum).

both Gaussian and polynomial methods usually gave physically meaningless ($z_{cf} < 0$) and/or impossible values (i.e., $z_{cf} > 40$ Å, well beyond the distance of the lipid polar headgroups from the center of the bilayer) when the quenching by 12SLPC or TempoPC is strongest ($z_{cf} < 9$ Å and $z_{cf} > 16$ Å).

The probable reason for the breakdown of the Gaussian and polynomial equations is illustrated in Figure 4. In this figure the effect of small deviations of quenching from a Gaussian depth dependence on calculated z_{cf} is illustrated. When the depths of the quenchers bracket the depth of a fluorophore, as shown in Figure 4a, small deviations in quenching from a Gaussian dependence of quenching have little effect on apparent z_{cf} (i.e., the depth at the minimum F/F_0). However, when the quenchers are all shallower or deeper than the fluorophore, then the smallest deviation of quenching from a Gaussian dependence of quenching on depth, or deviation due to a small experimental error, results in a very large error in calculated z_{cf} (Figure 4b). The parallax analysis does not suffer from these limitations, partly because it only uses the quenching of the two quenchers closest to the fluorophore to determine depth. It gives values in reasonable agreement with data obtained by methods other

than quenching, even in cases where fluorophores are very shallow or deep (see Discussion).

Comparison of Parallax Analysis and Double Gaussian Distribution Analysis. For deep fluorophores, quenching arises not only from quenchers that are in the same leaflet of the bilayer containing the fluorophore but also from the leaflet that does not contain the fluorescence group [trans leaflet quenching (1, 6)]. Recently a modified version of the distribution analysis (employing a double Gaussian) was proposed in which quenching of a fluorescence molecule arising from quenchers in both leaflets of the bilayer is taken into account (34).

Therefore, we compared the results of parallax analysis to that of the double Gaussian form of the distribution analysis (DGDA). Table 5 shows that DGDA never gives impossible negative depth values, but the depths obtained sometimes do not correspond well to those of parallax analysis, or to those derived from the single Gaussian distribution and polynomial analysis in the range of depths where they give reasonable values, with differences of 3 Å or more obtained in numerous cases. Several features of the DGDA results indicate that it is not giving depth as accurate as the other analyses in such cases. For example, DGDA reports an unusually shallow location for DPH ($z_{cf} = 12$ Å) which would place DPH at the same depth as TMA-DPH, which carries a charge directly attached to the phenyl ring. DGDA also reports a shallow depth for 9-anthroyloxy-stearate at pH 5 ($z_{cf} = 16$). This would place the 2, 6, and

⁵ However, it should be noted that, as described previously (3, 5), when 5SLPC quenches most strongly and $0.95 < F_{12SLPC}/F_{TempoPC} < 1.05$ it is necessary to average z_{cf} values with the TempoPC/5SLPC pair and 5SLPC/12SLPC pair in order to obtain the most accurate z_{cf} values using parallax analysis.

Table 5: Comparison of Average Depth of DPH Probes Determined by Different Quenching Analyses^a

fluorophore	Z_{cf} parallax	Z_{cf} distribution (double Gaussian)
DPH propionic acid (pH 10.0)	9.5	13.1
1,6-DPH	7.8	12.0
DPH-PC	6.9	6.4
DPH propionic acid (pH 4.5)	5.7	4.1
DPH propionic acid (pH 10.0) with cholesterol	9.2	13.9
1,6-DPH with cholesterol	6.7	4.3
DPH-PC with cholesterol	6.2	2.6
DPH propionic acid (pH 4.5) with cholesterol	4.6	2.7
anthracene	9.9	11.5
anthracenemethanol	12.7	14.3
anthracenemethyl	7.5	11.5
bisnorhydroxycholelate (AMC) acetate		
AMC oleate	12.6	14.1
anthracene propionic acid	10.0	13.4
anthracenylpropyl ammonium chloride	10.8	12.3
anthracenylpropyl trimethylammonium bromide	13.3	13.5
2-anthroyloxy stearate (pH 5)	15.8	17.2
2-anthroyloxy stearate (pH 10)	16.8	19.2
6-anthroyloxy stearate (pH 5)	12.3	15.3
6-anthroyloxy stearate (pH 10)	15	15.7
9-anthroyloxy stearate (pH 5)	8.8	16.2
9-anthroyloxy stearate (pH 10)	12.6	15.4
12-anthroyloxy stearate (pH 5)	6.0	6.6
12-anthroyloxy stearate (pH 10)	7.5	14.0
carbazole	15.1	15.0
11-carbazole undecanoic acid (pH 5)	7.5	11.2
11-carbazole undecanoic acid (pH 10)	10.6	13.3
indolebutyric acid	15.7	16.0
methylaminomethyl anthracene	12.5	12.4
methylanthracene	8.2	12.5
methyl anthracene propionate	9.4	12.4
methylcarbazole	13.4	14.1
NBD-PE	18.9	30.0
12-NBD-PC	19.8	73.4
octylphenol	14.1	14.6
TMA-DPH	10.9	12.4
TMAP-DPH	8.9	12.4
TMA-DPH with cholesterol	10.7	13.1
TMAP-DPH with cholesterol	8.2	11.2
tryptophan octyl ester	13.5	13.6

^a For the Gaussian analysis a coefficient of determination for the curve fitting very close to 1 was obtained in all cases except for DPH propionic acid at pH 4.5 (0.91–0.93) and 12 anthroyloxystearic acid (0.86).

9 anthroyloxy stearic acids at almost the same shallow depths, despite strong evidence to the contrary from several studies [(3), and references therein]. Another example is NBD probes, where DGDA gives depths too shallow ($Z_{cf} = 30\text{--}70\text{ \AA}$) to be physically possible. Finally, DGDA reports inconsistent effects for the effect of carboxyl group ionization on depth. Instead of the 1–4 \AA shallower depth of probes upon ionization reported by parallax analysis (3), DGDA reports a wide range of values for the change in depth upon ionization, from an 8–11 \AA shift to shallower locations for DPH propionic acid and 12-anthroyloxy stearic acid to a –1 \AA shift (9-anthroyloxy stearic acid) or no shift (6-anthroyloxy stearic acid) for very similar molecules. Such behavior seems very unlikely.

Associated with the most unlikely depths calculated from DGDA were values for the width of the depth distributions on the order of from 30 to over 50 \AA (not shown). Such distributions would place a significant population of hydrophobic fluorescent groups beyond the boundaries of the

bilayer. The origin of this problem may be that the distribution parameter is sensitive to the shape of the orbital containing the excited state electron giving rise to fluorescence. We believe the non-Gaussian shape of this electron distribution is likely to affect the DGDA analysis. Nevertheless, there are a significant number of cases in which DGDA will be very useful and accurate (see Discussion).

DISCUSSION

This study (1) has provided direct measurements of the location of the DPH probes in membranes, important because it allows more exact interpretation of the behavior of these widely used probes; (2) has allowed the formulation of general rules about the location of charged groups and acyl chains within bilayers (see below); and (3) has provided the first systematic comparison of different methods for analysis of quenching analysis. This is of great importance because the accuracy of calculated depths could depend on the method used, and an alternate method has been claimed to be superior to parallax analysis (see below).

Location of DPH Derivatives in Membranes. The DPH group has several properties that are likely to control its depth in membranes. The first is that it is a very hydrophobic group. This means that it would be expected to generally locate deeply within membranes. Its second property is that it is a long molecule with a C–C length of about 14 \AA . The third property is its rigid rodlike shape, which allows DPH to pack well with fatty acyl chains. This is illustrated by the ability of DPH to partition significantly into the ordered and tightly packed acyl chains found in the gel phase (35–37).

Together these properties can explain the depths we measured for the DPH derivatives. In all cases the DPH group was deeply buried, as expected from its hydrophobic nature. In general, the effect of derivitizing DPH with a charged anchoring group resulted in only a modest change in DPH depth. This is likely to be a result of the fact that DPH is long enough so that when aligned roughly parallel to the acyl chains its shallow end will be close to the membrane surface. A polar group can thus be accommodated at the shallow end of the molecule without involving a large change in DPH location.

The tendency to align parallel to acyl chains may also explain why, despite the fact it is a simple hydrocarbon, the free DPH molecule does not on the average locate at an extremely deep location within the bilayer. The portions of the acyl chains of lipids closer to the bilayer surface are better aligned than the portions toward the center of the bilayer, and DPH may pack better with this acyl chains in the region of the bilayer. We feel it is likely that the previously reported differences in fluorescence polarization of free and anchored forms of DPH *largely* reflect a direct effect of anchoring on motion, as suggested by the model of Engel and Prendergast (21), rather than due to the effect of anchoring on DPH location.

The Location of the Anchoring Groups and the Anchoring of Probes at Shallow or Deep Depths Are Determined by the Properties of the Anchoring Group. One significant concern when examining the location of anchoring groups, or their effect on fluorophore depth, is the extent to which the behavior observed is due to the fluorescent probe chosen.

The results of this report allow us to conclude for the first time that several phenomena we have previously observed are not due to the structure of the fluorescent probe.

The first set of observations concerns the location of anchoring groups. Charged carboxyl or quaternary nitrogen anchoring group attached to DPH locate near the membrane surface, about 19 Å from the center of the membrane. This value is within 1 Å of the depths found for ionized carboxyl groups on anthroyloxy fatty acid derivatives and quaternary nitrogen groups attached to anthracene probes (3, 4). The deeper location of the uncharged protonated carboxyl group of DPH propionic acid (15–16 Å from the bilayer center) is also in agreement with previous values (14–16 Å) obtained for anthroyloxy fatty acid and anthracene derivatives (3, 4). Thus, the location of these anchoring groups is largely dependent on their structure rather than that of the probe to which they are attached.

Another observation was that for DPH derivatives the 2-position fatty acyl location on PC is intermediate between the depth of protonated and ionized forms of the free fatty acid. The previous observation of similar behavior for carbazole-labeled fatty acids and a carbazole-PC derivative (38) suggests this reflects an intrinsic difference in depth between free fatty acids and fatty acyl chains of lipids.

Finally, we observed that attachment of DPH to an un-ionized propionic acid group actually results in deeper anchoring of the DPH group relative to free DPH. We previously noted a similar phenomenon for anthroyloxy (39) and carbazole groups when attached to fatty acids (5). However, the anthroyloxy and carbazole groups are more polar than DPH. We conclude the tendency of the acyl chain linker to align parallel to the acyl chains of the lipids results in a deeper fluorescent probe location, in a sense pushing both polar and nonpolar groups deeper within the bilayer. An alternate possibility is that the increased hydrophobicity resulting from the addition of a hydrophobic linker group results in a deeper location.

Comparison to Information about DPH Depth from Previous Studies. Previous studies have revealed some information about the relative location of DPH groups in membranes. Straume and Litman (14) studied the effects of cholesterol on membrane structure using DPH and TMA-DPH. They concluded from the effects of temperature and cholesterol on fluorescence lifetime that TMA-DPH is in an environment more likely to encounter water molecules than that of DPH, consistent with a shallower location for the former. Trotter and Storch (31) concluded that DPH-propionic acid located more deeply than TMA-DPH based on its longer lifetime and lesser sensitivity of lifetime to temperature. From the pH dependence of fluorescence intensity and polarization, they concluded it was likely that the ionized form of DPH propionic acid was located more shallowly than the protonated form. These conclusions are all in good agreement with our results. The relative locations of DPH and the DPH-propionic acid (at pH 7.4, where the latter should be partly ionized) were harder to define. From lifetime, free DPH seemed deeper, but by lifetime temperature sensitivity, it seemed shallower than DPH propionic acid. Ferrati et al. (16) concluded from a small red shift in excitation and lifetime measurements that DPH-PC (which contains DPH propionic acid attached to the 2-position of PC) located at a depth close to TMA-DPH. This result is

hard to reconcile both with our results and the behavior of DPH-propionic acid noted above. It seems unlikely that attachment to PC would result in a very shallow location for the DPH group.

These studies show that some information about the depth of DPH groups can be obtained from various fluorescence properties, but such properties cannot pinpoint the depth of the DPH group because they are likely to reflect various factors. The direct determination of depth from quenching should allow more detailed analysis of membrane dynamics from DPH derivatives, by separating effects due to differences in depth from other variables.

Cholesterol Effects on Quenching and Depth. As noted in Results, the most striking effect of cholesterol was that it increased the differences between the levels of quenching by nitroxides at different depths. This effect has been seen previously with brominated lipid quenching of pyrene-labeled lipids (33), and can be explained by the fact that cholesterol increases bilayer thickness as the acyl chains become more extended (27, 33). This increases the differences between the depths of different quenchers and thus differences in quenching.⁵ Reduced vertical (transverse) motion in the presence of cholesterol may also contribute to this effect.

Cholesterol can also greatly influence the depth of molecules in membranes (6). However, cholesterol had little effect on the depths of DPH probes. This suggests that cholesterol-induced effects on DPH fluorescence polarization also primarily reflect changes in DPH motion, not DPH location, although additional studies with other cholesterol-containing lipid mixtures would be required to extend this conclusion.

Evidence That Parallax Analysis Is the Most Accurate Method for Analysis of Quenching in Many Cases. A second important aim of this report was to compare the different methods for calculating depth from fluorescence quenching. The original method to determine depth from quenching was to compare the amount of quenching induced by a series of several nitroxide-labeled (or brominated) lipids at various depths. Fluorophore depth was identified as being closest to that of the most strongly quenching nitroxide (or bromine) group [see reviews (40, 41)]. This method was not useful when the fluorophore was shallower or deeper than all of the quenchers used. Parallax analysis was designed to allow more precise pinpointing of average depth with a minimum number of quenchers (1, 3). More recently, methods have been introduced to Gaussian curve fit the dependence of quenching on quencher depth and then determine the depth at which quenching would be a maximum, which is the depth of the fluorophore (28, 32, 33). It has been suggested that such methods should be generally superior to the parallax analysis (28, 32).

As noted in Results, there is good agreement between average depths derived by parallax and curve-fitting methods for a wide variety of molecules where the strongest quenching is obtained with the middle depth quencher (5SLPC). However, curve fitting methods do not work well when a fluorophore is shallow or deep, i.e., cases in which the strongest quenching is by the shallowest or deepest quencher, respectively. It is likely that curve-fitting methods may be inadequate under these conditions because the quenching function progressively deviates from a Gaussian or second-

order polynomial as the difference between fluorophore and quencher depth increases (see Results).

Another problem for curve-fitting methods will occur when there is a second population of fluorophores at an average depth different from that of the first population. Examples of such behavior have been observed both for small molecules (42) and proteins (43). Such cases give multiple quenching maxima vs depth, and thus cannot fit a single Gaussian. It would be possible to fit such data to multiple Gaussian curves, but when three nitroxide-labeled quenchers are used there is insufficient information for such a fit. Quenchers at five depths would be needed. Thus, additional quenchers covering a wider range of depths will be needed to solve both these limitations. We conclude that at present, parallax analysis is the most accurate method for analysis of quenching for the widest range of cases.

Furthermore, the parallax analysis has now been applied to a large number of fluorescent molecules so it is also possible to assess its accuracy more fully through the degree of agreement between quenching results and other methods. Although there is generally little precise information available from other methods good agreement has been obtained between depths estimated by parallax analysis and energy transfer (anthroyloxy and NBD), thermodynamic considerations (trp analogues), aqueous quenching (dansyl, NBD, anthroyloxy, Trp analogues), and emission maxima (NBD and dansyl) (1–4, 42, 44).

Perhaps the most direct results in this regard have been obtained with a series of transmembrane helices with Trp residues at various defined positions along the helix. This is a useful system because of the relatively fixed geometry of an α -helix. In this case, parallax analysis appears to be accurate to within 1–2 Å (6).

Advantages of Quenching Analysis Using Curve Fitting Methods. It is important to note curve fitting analysis methods also have important advantages over parallax analysis in certain situations. For example, in cases where averaging of z_{cf} for the TempoPC/5SLPC pair and 5SLPC/12SLPC pair is needed (i.e., where quenching is strongest by 5SLPC and nearly equal for TempoPC and 12 SLPC) for calculation of accurate values by parallax analysis (3), no such averaging is needed for curve fitting methods. Another advantage is that they should not be affected by the presence of a background fluorescence arising from unbound probe molecules in aqueous solution (32). To avoid this problem with parallax analysis, quenching is measured under conditions in which fluorescence arises only from membrane-bound molecules, and/or is performed only after correcting for the amount of fluorescence arising from solution (5). Another advantage of curve fitting methods is that they work well for long-lifetime fluorophores, in which motions during the excited state lifetime affect quenching (2, 33). A third advantage may be in cases of restricted lateral approach of quenchers to a fluorescent group to a very large molecule (32). This can interfere with parallax analysis (not shown). Also, curve fitting methods can potentially provide information about the distribution, motion, and/or orientation of fluorescent molecules in addition to average fluorophore depth (28, 33). If additional quenchers covering a wider range of depths are developed, curve fitting methods could become the method of choice for analysis of quenching in a significant number of cases. The

double Gaussian distribution analysis is likely to be especially useful in cases in which the dependence of quenching on depth is very strong and the fluorophore is not too large (so that the maximum intrinsic depth distribution of its electron density is small). This is likely to be the case when brominated lipids, which have a shorter range of quenching than nitroxides, are used to examine depths of Trp residues.

ACKNOWLEDGMENT

The authors thank Michael Rosconi for the calculation of DPH length.

REFERENCES

1. Chattopadhyay, A., and London, E. (1987) *Biochemistry* 26, 39–45.
2. Abrams, F. S., and London, E. (1992) *Biochemistry* 31, 5312–5322.
3. Abrams, F. S., and London, E. (1993) *Biochemistry* 32, 10826–10831.
4. Asuncion-Punzalan, E., and London, E. (1995) *Biochemistry* 34, 11460–11466.
5. Kachel, K., Asuncion-Punzalan, E., and London, E. (1995) *Biochemistry* 34, 15475–15479.
6. Ren, J., Lew, S., Wang, Z., and London, E. (1997) *Biochemistry* 36, 10213–10220.
7. Palmer, L. R., and Merrill, A. R. (1994) *J. Biol. Chem.* 269, 4187–4193.
8. Ramalingam, T. S., Puspendu, K. D., and Podder, S. K. (1994) *Biochemistry* 33, 12247–12254.
9. Chung, L. A., Lear, J. D., and De Grado, W. F. (1992) *Biochemistry* 31, 6608–6616.
10. Jones, J. D., and Gierasch, L. M. (1994) *Biophys. J.* 67, 1534–1545.
11. Fiorini, R., Valentino, M., Wang, S., Glaser, M., and Gratton, E. (1987) *Biochemistry* 26, 3864–3870.
12. Lentz, B. R. (1989) *Chem. Phys. Lipids* 50, 171–190.
13. Lentz, B. R., Wu, J. R., Zheng, L., and Prevratil, J. (1996) *Biophys. J.* 71, 3302–3310.
14. Straume, M., and Litman, B. J. (1987) *Biochemistry* 26, 5121–5126.
15. Lentz, B. R. (1993) *Chem. Phys. Lipids* 64, 99–116.
16. Ferretti, G., Tangorra, A., Zolese, G., and Curatola, G. (1993) *Membr. Biochem.* 10, 17–27.
17. Zolese, G., Gratton, E., and Curatola, G. (1990) *Chem. Phys. Lipids* 55, 29–39.
18. Antunes-Madeira, M. C., Videira, R. A., Kluppel, M. L. W., and Madeira, V. M. C. (1995) *Int. J. of Cardiol.* 48, 211–218.
19. Simonetti, O., Ferretti, G., Offidani, A. M., Gervasi, P., Curatola, G., and Bossi, G. (1996) *Arch. Dermatol. Res.* 288, 51–54.
20. Haugland, R. P. (1996) *Handbook of Fluorescent Probes and Research Chemicals* (K. D. Larison, Ed.) 6th ed., Molecular Probes, Inc., Eugene, OR.
21. Engel, L. W., and Prendergast, F. G. (1981) *Biochemistry* 20, 7338–7345.
22. Prendergast, F. G., Haugland, R. P., and Callahan, P. J. (1981) *Biochemistry* 20, 7333–7338.
23. Konopasek, I., Kvasnicka, P., Amler, E., Kotyk, A., and Curatola, G. (1995) *FEBS Lett.* 374, 338–340.
24. Bernsdorff, C., Wolf, A., Winter, R., and Gratton, E. (1997) *Biophys. J.* 72, 1264–1277.
25. Kachel, K., Asuncion-Punzalan, E., and London, E. (1998) *Biochim. Biophys. Acta* (in press).
26. Engelman, D. M., and Rothman, J. E. (1972) *J. Biol. Chem.* 247, 3694–3697.
27. Ipsen, J. H., Mouritsen, O. G., and Bloom, M. (1990) *Biophys. J.* 57, 405–412.
28. Ladokhin, A. S., and Holloway, P. W. (1996) *Biophys. J.* 69, 506–517.

29. Engel, L. W., and Prendergast, F. G. (1981) *Biochemistry* 26, 7338–7345.
30. Green, S. A., Simpson, D. J., Zhou, G., Ho, P. S., and Blough, N. V. (1990) *J. Am. Chem. Soc.* 112, 7337–7346.
31. Trotter, P. J., and Storch J. (1989) *Biochim. Biophys. Acta* 982, 131–139.
32. Ladokhin, A. S. (1997) *Biophys. J.* 72, a121.
33. Sassaroli, M., Ruonala, M., Virtanen, J., Vauhkonen, M., and Somerharju, P. (1995) *Biochemistry* 34, 8843–8851.
34. Ladokhin, A. (1997) *Methods Enzymol.* 278, 462–473.
35. Florine-Casteel, K., and Feigenson, G. W. (1988) *Biochim. Biophys. Acta* 941, 102–106.
36. Lentz, B. R., Barenholz, Y., and Thompson, T. E. (1976) *Biochemistry* 15, 4529–4537.
37. London, E., and Feigenson, G. W. (1981) *Biochim. Biophys. Acta* 649, 89–97.
38. Abrams, F. S., Chattopadhyay, A., and London, E. (1992) *Biochemistry* 31, 5322–5327.
39. Waggoner, A. S., and Stryer, L. (1970) *Proc. Natl. Acad. Sci. U.S.A.* 67, 579–589.
40. London, E. (1982) *Mol. Cell. Biochem.* 45, 181–188.
41. Blatt, E., and Sawyer, W. H. (1985) *Biochim. Biophys. Acta* 822, 43–62.
42. Asuncion-Punzalan, E., Kachel, K., and London, E. (1998) *Biochemistry* 37, 4603–4611.
43. Wang, Y., Malenbaum, S. E., Kachel, K., Zhan, H., Collier, R. J., and London, E. (1997) *J. Biol. Chem.* 272, 25091–25098.
44. Chattopadhyay, A., and London, E. (1988) *Biochim. Biophys. Acta* 938, 24–34.

BI980064A